

# Theoretical and experimental aspects of enantiomeric differentiation using natural abundance multinuclear nmr spectroscopy in chiral polypeptide liquid crystals

Muriel Sarfati, Philippe Lesot,\* Denis Merlet and Jacques Courtieu\*

Laboratoire de Chimie Structurale Organique, Université de Paris-Sud, Bât. 410, ICMO CNRS ESA n°8074, 91405 Orsay cedex, France. E-mail: philesot@icmo.u-psud.fr; courtieu@icmo.u-psud.fr

Received (in Liverpool, UK) 1st August 2000, Accepted 16th August 2000  
First published as an Advance Article on the web 18th September 2000

Liquid crystalline organic solutions of poly- $\gamma$ -benzyl-L-glutamate generate a sufficient differential ordering effect to visualize enantiomers using multinuclear high-resolution NMR spectroscopy at natural isotopic abundance levels. Chiral discrimination can be observed through a difference in the order-sensitive NMR observables, namely: proton–proton, carbon–proton and carbon–carbon residual internuclear dipolar couplings, carbon chemical shift anisotropies, and deuterium quadrupolar splittings. In most cases, the enantiodifferentiation

is large enough to allow determination of the enantiomeric excesses satisfactorily. All theoretical considerations and significant experimental parameters that affect the efficiency of this methodology are presented and discussed. The various possible anisotropic NMR techniques provide a very reliable and powerful alternative to the current analytical techniques which operate in the isotropic phase.

## Introduction

The sustained interest in enantioselective synthesis and the necessity of providing reliable quality control tests for marketed or new candidate synthetic chiral drugs in the pharmaceutical industry, have strongly stimulated the development of novel, convenient and efficient techniques for enantiomeric purity analysis. Among them NMR spectroscopy is widely used. Various NMR methods using isotropic solvents, nicely reviewed by Parker,<sup>1,2</sup> are available for determining enantiomeric excesses (ee's), but all suffer of a lack of generality. For instance, derivatization of chiral molecules using chiral derivatizing agents requires the presence of a reactive function and great care is required to ensure that neither kinetic resolution nor racemization occur during the derivatization. The preparation of specific complexing agents is needed when using chiral solvating agents dependent on the functional groups in the chiral molecule under study. Also the use of chiral lanthanide shift reagents works only when the enantiomers may complex the paramagnetic center in equilibrium at the NMR timescale. Last, but not least, the final result is not always satisfactory as in almost all cases, only the variation of a chemical shift is utilised for discriminating between isomers.

To provide an alternative when usual isotropic NMR methods fail and to avoid some of their main disadvantages, we have developed an analytical approach based on the use of chiral liquid crystals (CLC). The best results, to date, have been obtained with a chiral anisotropic solvent comprised of a synthetic polypeptide, poly- $\gamma$ -benzyl-L-glutamate (PBLG), dissolved in various organic solvents such as chloroform, dichloromethane, dimethyl formamide, *etc.*<sup>3–6</sup>

NMR spectra of chiral solutes in this liquid crystalline medium are extremely rich in their information because they are affected not only by the usual scalar couplings and chemical shifts, but also by anisotropic interactions such as dipolar couplings, chemical shift anisotropy (CSA) and if the nuclei have a spin  $I > 1/2$ , by quadrupolar interactions. It is differences in these anisotropic interactions which provide the chiral discrimination. We have shown that this effect originates from the fact that enantiomers are not oriented in the same manner in this chiral anisotropic medium. The great advantage that this new NMR analytical method has over the more established techniques, which use isotropic solvents, is that

---

Muriel Sarfati was born in Saint Denis, France, in 1974. She received her degree in chemistry in 1998 and is now doing a Ph.D at the University of Paris XI with Dr. P. Lesot and Professor J. Courtieu on natural abundance deuterium NMR spectroscopy in oriented solvents.

Philippe Lesot has been a scientific researcher at the CNRS since 1998. He was born in Paris, France, in 1967. He did his Ph.D at the University of Paris XI under the supervision of Professor J. Courtieu (1992–95). He then received a post-doctoral grant from the Royal Society of Chemistry and joined the Professor J. W. Emsley's NMR group at the Chemistry Department of the University of Southampton (1995–96). In 1997–98 he was appointed as lecturer in Chemistry at the University of Paris XI.

Denis Merlet was born in Etampes, France, in 1970. He received his Ph.D from the University of Paris VII in 1998 (Professor J. Courtieu). He was a postdoctoral fellow of the French Foreign Office and spent one year with the NMR group of Professor J.W. Emsley at Southampton (1998–99). In 1999 he returned to the University of Paris XI to take up his present position as a lecturer in Chemistry.

Jacques Courtieu is Professor of Chemistry at the University of Paris XI since 1983. He was born in Saint-Marcellin, France, in 1944. He sustained a Ph.D thesis at the University of Paris XI (Professor J. Jullien), and subsequently was a postdoctoral fellow of the University of Utah, Salt Lake City, for two years with Professor D. M. Grant's NMR team (1976–78). He is currently Chairman of the Orsay Institute for Molecular Chemistry (I.C.M.O.). In 1999, he has received the Grammaticakis-Neuman award from the French Academy of Sciences.

The research interests of the authors focus mainly on the design and the development of new NMR methodologies using oriented solvents with applications in structural chemistry. Their current work includes the enantiodifferentiation of chiral molecules using 1 D and 2 D NMR spectroscopy in chiral liquid-crystalline media.

chiral discrimination can be achieved for a very wide range of compounds, including those in which there are no functional groups, such as saturated hydrocarbons. A second important advantage is that there are a number of NMR nuclei which can be exploited, and for a specific molecule there are usually many NMR parameters which can be measured, with varying sensitivities to chirality. In this review, we will illustrate this point through the investigation of a single chiral compound, ( $\pm$ )-1-chloropropan-2-ol [( $\pm$ )-CP] for which we will show that it is possible to discriminate its *S* and *R* isomers using proton, carbon-13 and deuterium NMR spectroscopy, the enantiodifferentiation being based on a difference in their  $^1\text{H}$ - $^1\text{H}$ ,  $^1\text{H}$ - $^{13}\text{C}$  residual dipolar couplings, carbon-13 CSA or  $^2\text{H}$  residual quadrupolar splittings. In addition we will report the first successful enantiomeric discrimination based on differences of  $^{13}\text{C}$ - $^{13}\text{C}$  residual dipolar couplings.

To introduce chemists to this non-conventional area of NMR spectroscopy, all essential theoretical and practical aspects of NMR in chiral anisotropic solvents, particularly when using the PBLG system, are reviewed. Consequently, this article is not a comprehensive survey of successful results already obtained using this methodology, but is rather intended to describe and assess the respective practical interests of various 1D and 2D multinuclear NMR tools in natural isotopic abundance systems that have been used or specifically developed to visualize enantiomers dissolved in the PBLG phase. Thus, all experimental parameters or useful details that can affect the efficiency of each of the NMR tools proposed will be examined and discussed. It is important to emphasise that all NMR spectra of ( $\pm$ )-CP reported in this work were obtained in natural isotopic abundance.

## NMR in chiral oriented solvents: background

Since the pioneering work of Snyder and coworkers, it is known that enantiomers may give different NMR spectra when dissolved in a chiral anisotropic material.<sup>7,8</sup> This situation arises because the difference in the enantioselective interactions between the *S* and *R* isomers and the CLC generally generates a sufficient differential ordering effect (DOE) to discriminate between them using order-sensitive NMR observables.<sup>9,10</sup> These various observables, which are averaged to zero due to the isotropic motion of solutes in the liquid state, are the chemical shift anisotropy, ( $\Delta\sigma_i$ ), the spin-spin coupling anisotropy ( $\Delta T_{ij}$ ) and the quadrupolar splitting for spin  $I > 1/2$  nuclei ( $\Delta\nu_Q$ ).<sup>11</sup> It should be noted that ( $\Delta T_{ij}$ ) is due to the purely anisotropic dipolar couplings ( $D_{ij}$ ) and to the anisotropy of the scalar coupling, ( $\Delta J_{ij}$ ), the latter being generally considered small in comparison to  $D_{ij}$ . In the following, we will assume that  $\Delta J_{ij}$  is negligible, thus reducing  $\Delta T_{ij}$  to  $D_{ij}$ . A rough classification of the sensitivity of these anisotropic interactions towards the DOE of enantiomers indicates that  $|\Delta\nu_Q| > |\Delta T_{ij}| > |\Delta\sigma_i|$ .<sup>11</sup>

The analysis of NMR spectra obtained in CLC differs from their isotropic analogues, but the numerous anisotropic interactions provide interesting tools as far as enantiodiscrimination is concerned. Regarding the various active NMR nuclei intrinsically included in any chiral organic compounds and their natural magnetic properties, namely,  $^1\text{H}$  ( $I = 1/2$ , 99.985%),  $^{13}\text{C}$  ( $I = 1/2$ , 1.108%) and  $^2\text{H}$  ( $I = 1$ , 0.015%), it appears that, theoretically, there are ten possible NMR observables for detecting the DOE, namely  $\Delta\sigma_{\text{H}}$ ,  $\Delta\sigma_{\text{C}}$ ,  $\Delta\sigma_{\text{D}}$ ,  $\Delta T_{\text{HH}}$ ,  $\Delta T_{\text{HD}}$ ,  $\Delta T_{\text{DD}}$ ,  $\Delta T_{\text{CC}}$ ,  $\Delta T_{\text{CH}}$ ,  $\Delta T_{\text{CD}}$  and  $\Delta\nu_{\text{QD}}$ . However, some of these will not provide an efficient tool for our purpose because the weakness of the natural isotopic abundance of the involved nuclei. For instance, the present sensitivities of routine spectrometers do not permit the observation of  $\Delta T_{\text{CD}}$  or  $\Delta T_{\text{DD}}$ , in natural abundance NMR. In contrast, when enantiomers under investigation exhibit other X-active nuclei of spin  $I = 1/2$  (fluorine-19, phosphorus-31, ...) or  $I > 1/2$  (boron-10, boron-

11, ...), additional NMR observables such as  $\Delta\sigma_{\text{X}}$ ,  $\Delta T_{\text{HX}}$ ,  $\Delta T_{\text{CX}}$  or  $\Delta\nu_{\text{QX}}$  are available and therefore increase the probability to reveal an enantiomeric discrimination.<sup>12,13</sup> Finally, as all these anisotropic NMR interactions are order-sensitive and therefore temperature-, concentration- and solvent-dependent, we have three further variables at our disposal to control the DOE, thus enhancing the probability to detect a chiral differentiation. Consequently, this analytical strategy offers undoubtedly better possibilities for discriminating between enantiomers compared with current isotropic NMR techniques in which only the variation of a chemical shift is used.<sup>1,2</sup> As we will show throughout this work, the two main features of this non-conventional approach generally involving a single NMR sample preparation are, therefore, both its analytical potentialities and high adaptability from the NMR point of view.

## Description of the chiral liquid crystalline solvent

The chiral recognition principle in the liquid crystalline state is based on the ability for the chiral phase to orientate differently the two enantiomers as schematically depicted in Fig. 1, and so the choice of the solvent is crucial.<sup>8,9,14,15</sup> As a consequence, we need to have a system able to interact enantioselectively with almost all enantiomers (functionalized or not) and give sufficiently large orientational differences which can be revealed using NMR spectroscopy. This condition supposes therefore that the enantioselective electrostatic interactions as well as geometric shape recognition play an important role in the discrimination mechanisms. Actually, this situation is very similar to that involved for enzymatic enantioselectivity in biological systems.

From the NMR point of view, the liquid crystal should ideally solubilize almost all organic compounds, provide a very homogeneous anisotropic mesophase with low viscosity at about room temperature, and its NMR spectrum should not interfere with that of the dissolved molecules. In addition, the DOE is not directly related with the magnitude of orientational order parameters and in fact it is advantageous to use an anisotropic solvent exhibiting low molecular ordering for solutes. This is firstly because in the majority of cases the proton and proton-coupled X spectra can be easily analysed in a similar way as for isotropic spectra. Second, the contribution to NMR linewidths of order inhomogeneities in the sample is rather small, hence a higher signal-to-noise (*S/N*) ratio may be achieved. This is a key point to observe chiral discriminations for very low-sensitive quadrupolar nuclei such as deuterons at natural abundance level.<sup>16-18</sup>

Among the CLC examined up to now, the most valuable mesophase satisfying all criteria mentioned above is the lyotropic system poly- $\gamma$ -benzyl-L-glutamate (PBLG) or its enantiomer poly- $\gamma$ -benzyl-D-glutamate (PBDG), in solution with various organic helicogenic co-solvents.<sup>19-22</sup> In such co-solvents, the main chain of the synthetic homo-polypeptide adopts a rigid  $\alpha$ -helical conformation similar to that observed for some naturally occurring polypeptides<sup>23</sup> while the glutamate side chains, which branch from the main helix, also form a secondary molecular helix.<sup>22,24-26</sup>

Within a certain concentration range, organic solutions of PBLG are liquid crystals. Spontaneously, the PBLG chiral fibers orientate to form a macroscopic, supramolecular helical structure of directors in the mesophase, typical of that exhibited by cholesteric liquid crystals. However, when submitted to a routine NMR magnetic field, the supramolecular helix unwinds, and the system behaves like a chiral nematic phase with positive anisotropy of the molecular diamagnetic susceptibility ( $\Delta\chi_{\text{m}} > 0$ ), with the director, *n*, homogeneously aligned parallel to the static magnetic field  $B_0$  (Fig. 1).<sup>27,28</sup> Various possible co-organic solvents may be used. Chloroform, dichloromethane, dioxane, DMF and THF are among the most convenient to dissolve a wide variety of organic materials.<sup>24,29,30</sup> However,

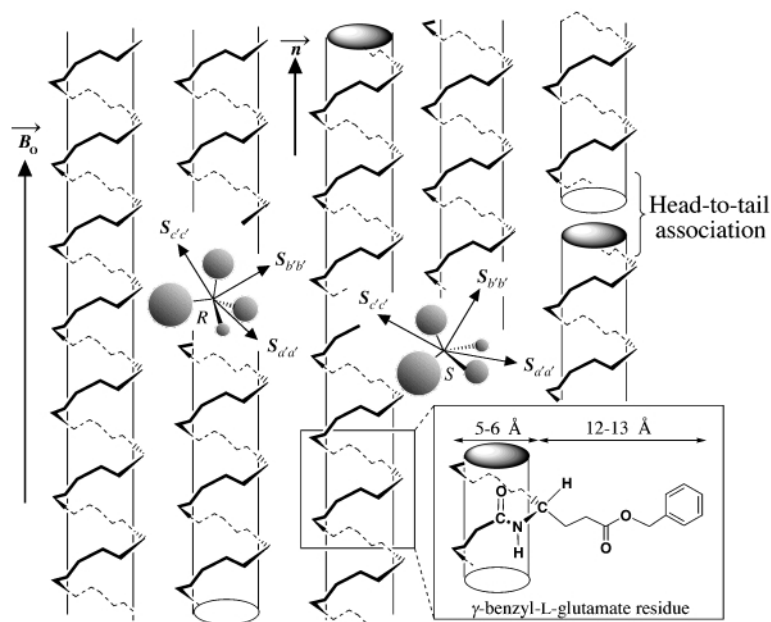


**Fig. 1** Schematic illustration of the differential ordering effect for two enantiomers dissolved in the PBLG phase. To clarify the drawing, the glutamate side chains of the polypeptide and the co-solvent molecules were not displayed. The assignments *S* and *R* and the space representation of the orientational principal axis system (*a'*, *b'*, *c'*) of enantiomers should be regarded as arbitrary. The PBLG and chiral solutes are not plotted to scale. Note the head-to-tail associations between two PBLG fibers.

for DMF or dioxane, it is necessary to heat the mixture in order to dissolve the polymer during the sample preparation. In all cases the organic co-solvent employed has to homogeneously dissolve the polypeptide and preserve the  $\alpha$ -helical structure of the polymer. For instance, trifluoroacetic acid and DMSO are not suitable co-solvents since they form strong intermolecular hydrogen bonds with the polypeptide chain, giving rise to a random coil conformation for the PBLG, and consequently, the liquid crystalline properties of the solvent disappear.<sup>24</sup> Studies for the optimisation of the ternary mixture, 'PBLG/co-solvent/chiral material', have established that the best NMR results are generally obtained for samples prepared with a concentration in PBLG which varies between 12 and 25% by weight. Except for molecules that are able to precipitate the PBLG fibers, the addition of a reasonable amount of solute (1–20%) in PBLG/co-solvent mixtures does not disrupt the liquid crystalline properties of the solvent. The average molecular weight of PBLG is another important factor for the quality of the enantiodiscrimination. Indeed, this parameter as well as the concentration of the polymer and the nature of the organic co-solvent determine the sample viscosity. Using the same co-solvent and keeping the PBLG concentration constant, the viscosity of the phase significantly decreases when the molecular weight of the polymer is reduced. Generally, a greater fluidity of the liquid crystalline phase provides longer transversal relaxation times for solutes ( $T_2^*$ ), and hence a better spectral resolution and *S/N* ratio. Therefore, we suggest using a PBLG whose degree of polymerisation (DP) is in the range 350–600.<sup>4,5</sup> Under these conditions, the sample temperature can be optimized between 285 and 340 K depending on both the organic co-solvent used and the solute under investigation. Finally we note that a DP below 200 is not convenient for our purpose because the liquid crystal range of the sample is either too small or non-existent.

## Theoretical considerations

### Analysis of the order-dependent NMR observables involved in chiral differentiation

When embedded in a liquid crystal, solute molecules are partially ordered.<sup>11</sup> This situation arises also using chiral liquid crystals, but in this case, the difference of interactions between

the enantiomers and the PBLG molecules generally produces a measurable difference in their orientational ordering.<sup>8,9,31</sup> Consequently, the molecular order of *S* and *R* isomers must be described by two distinct second-rank order tensors,  $S^S$  and  $S^R$ , denoted Saupe matrices, whose elements can be expressed as:<sup>11</sup>

$$S_{\alpha\beta}^{S \text{ or } R} = \frac{1}{2} \langle 3 \cos \theta_{\alpha_z}^{S \text{ or } R} \cos \theta_{\beta_z}^{S \text{ or } R} - \delta_{\alpha\beta}^{S \text{ or } R} \rangle \quad (1)$$

In this equation,  $\alpha, \beta = a, b, c$  are the axes of the molecular fixed reference frame,  $\theta_{\alpha_z}^{S \text{ or } R}$  is the angle between the magnetic field and the molecule fixed  $\alpha$  axis in the *S* or *R* isomers (the *z* laboratory axis is assumed parallel to the  $B_0$  axis).  $\delta_{\alpha\beta}$  is the Kronecker symbol (unity if  $\alpha = \beta$  and zero otherwise). The angular brackets denote a statistical average over all orientations of the molecule as well as over all intramolecular motions. From the components of  $S^{S \text{ or } R}$ , we can derive the order parameter,  $S_{ij}^{S \text{ or } R}$ , of any direction along a vector  $v_{ij}$  in the molecular axis system (*a, b, c*):

$$\begin{aligned} S_{ij}^{S \text{ or } R} &= \sum_{\alpha, \beta = a, b, c} \cos \theta_{ij\alpha}^{S \text{ or } R} \cos \theta_{ij\beta}^{S \text{ or } R} S_{\alpha\beta}^{S \text{ or } R} \\ &= \frac{1}{2} (3 \cos^2 \theta_{ija}^{S \text{ or } R} - 1) S_{aa}^{S \text{ or } R} \\ &\quad + \frac{1}{2} (\cos^2 \theta_{ijb}^{S \text{ or } R} - \cos^2 \theta_{ijc}^{S \text{ or } R}) (S_{bb}^{S \text{ or } R} - S_{cc}^{S \text{ or } R}) \\ &\quad + 2 (\cos \theta_{ija}^{S \text{ or } R} \cos \theta_{ijb}^{S \text{ or } R}) S_{ab}^{S \text{ or } R} \\ &\quad + 2 (\cos \theta_{ija}^{S \text{ or } R} \cos \theta_{ijc}^{S \text{ or } R}) S_{ac}^{S \text{ or } R} \\ &\quad + 2 (\cos \theta_{ijb}^{S \text{ or } R} \cos \theta_{ijc}^{S \text{ or } R}) S_{bc}^{S \text{ or } R} \end{aligned} \quad (2)$$

where the  $\cos \theta_{ij\alpha}^{S \text{ or } R}$  are the director cosines of the vector  $v_{ij}$  in the molecular fixed frame. All the order-dependent NMR interactions are related to these order parameters as we will see in the next sections.

As a consequence of the DOE and of the non-zero averaging of order-dependent NMR interactions, the total static spin-Hamiltonian which describes the NMR spectra of each diamagnetic enantiomer in CLC must be written as the sum of four distinct terms:

$$\mathcal{H}_{\text{tot}}^{S \text{ or } R} = \mathcal{H}_{\text{cs}}^{S \text{ or } R} + \mathcal{H}_{\text{J}}^{S \text{ or } R} + \mathcal{H}_{\text{D}}^{S \text{ or } R} + \mathcal{H}_{\text{Q}}^{S \text{ or } R} \quad (3)$$

where  $\mathcal{H}_{\text{cs}}^{S \text{ or } R}$  is the Zeeman term including the electronic shielding contribution,  $\mathcal{H}_{\text{J}}^{S \text{ or } R}$  and  $\mathcal{H}_{\text{D}}^{S \text{ or } R}$  are the indirect electron-coupled and direct through-space spin-spin interactions and  $\mathcal{H}_{\text{Q}}^{S \text{ or } R}$  is the quadrupolar interaction caused by electric field gradients acting on quadrupolar nuclei ( $I > 1/2$ ). In this respect, magnetic interactions for liquid crystalline solutions are not different from those of solid state NMR, except that molecules are free to diffuse and tumble, leading to line narrowing, and hence high resolution spectra.

Let us now treat in detail the various order-dependent NMR observables involved in the analysis of NMR spectra of enantiomers in chiral anisotropic media.

### Chiral discrimination arising from chemical shift anisotropy

In a chiral anisotropic solvent, the resonance frequency  $\nu_i$  of a nucleus  $i$  contains both an isotropic,  $\sigma_i^{\text{iso}}$ , and an anisotropic,  $\Delta\sigma_i$ , contribution to the electronic shielding and may be written for two enantiomers such as:<sup>11</sup>

$$\nu_i^{R \text{ or } S} = \frac{\gamma}{2\pi} [1 - \sigma_i^{\text{iso}} - \Delta\sigma_i^{S \text{ or } R}] B_0 \quad (4)$$

Expressed in a molecular frame ( $a, b, c$ ), the terms  $\sigma_i^{\text{iso}}$  and  $\Delta\sigma_i$  at the  $i$ th site are defined as:

$$\sigma_i^{\text{iso}} = \frac{1}{3}(\sigma_{iaa} + \sigma_{ibb} + \sigma_{icc}) \text{ and}$$

$$\Delta\sigma_i^{S \text{ or } R} = \frac{2}{3} \sum_{\alpha, \beta = a, b, c} \sigma_{i\alpha\beta} S_{\alpha\beta}^{S \text{ or } R} \quad (5)$$

Eqn. (4) indicates clearly that chiral discrimination is detected in NMR spectra when  $\nu_i^S - \nu_i^R \neq 0$  as depicted in Fig. 2(a), *i.e.* when  $\Delta\sigma_i^S$  significantly differs from  $\Delta\sigma_i^R$ . However, the quantity

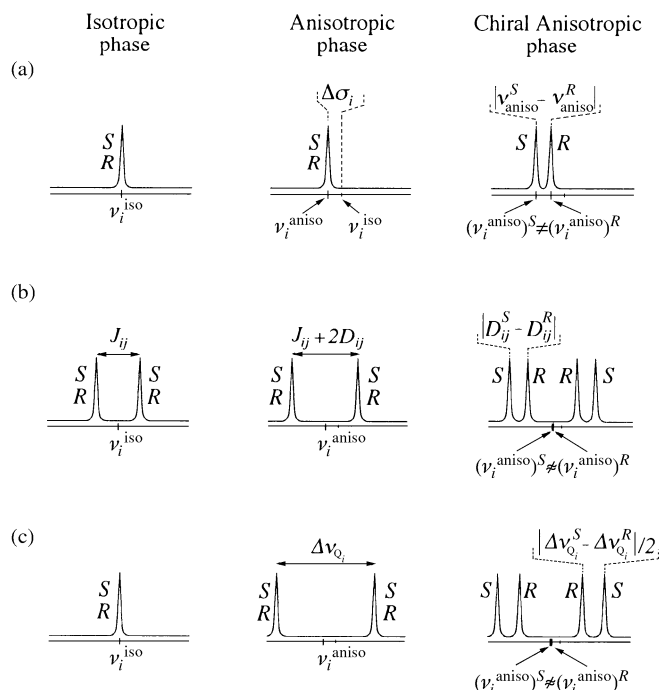


**Fig. 2** Principle of the enantiomeric discrimination in CLC based on (a) a difference of chemical shift anisotropies,  $\Delta\sigma_i$ , (b), residual dipolar couplings,  $D_{ij}$ , and (c) residual quadrupolar splittings,  $\Delta\nu_{\text{Q}}$ , for  $I = 1$  nuclei (deuterium). For all examples, we have assumed that  $\Delta\sigma_i$  was negative. In addition (b) and (c) are depicted assuming the CSA difference ( $\Delta\sigma_i^S - \Delta\sigma_i^R$ ) between the enantiomers in the chiral anisotropic phase was negligible.  $D_{ij}^S$  and  $D_{ij}^R$  were chosen to be smaller than  $J_{ij}$ , and having a positive and negative sign, respectively.  $\Delta\nu_{\text{Q}}$  can be positive or negative. The various spectra are not plotted to scale. The assignments  $S$  and  $R$  given in all spectra are arbitrary.

$\Delta\sigma_i^{S \text{ or } R}$  is not trivial to analyse as from eqn. (5) it depends both on the elements of the shielding tensor and on the orientational order parameters,  $S_{\alpha\beta}^{S \text{ or } R}$ , in the same reference frame. In order to consider the various factors governing this quantity, it is more convenient to recast the previous equation into:

$$\Delta\sigma_i^{S \text{ or } R} = \frac{2}{3} \left[ \sigma_{iaa} - \frac{1}{2}(\sigma_{ibb} + \sigma_{icc}) \right] S_{aa}^{S \text{ or } R}$$

$$+ \frac{1}{3}(\sigma_{ibb} - \sigma_{icc}) (S_{bb}^{S \text{ or } R} - S_{cc}^{S \text{ or } R}) \quad (6)$$

$$+ \frac{4}{3} (\sigma_{iab} S_{ab}^{S \text{ or } R} + \sigma_{iac} S_{ac}^{S \text{ or } R} + \sigma_{ibc} S_{bc}^{S \text{ or } R})$$

For each nucleus  $i$  of both enantiomers, there exists a principal frame ( $a', b', c'$ ), where the chemical shift tensor is diagonal. Consequently the relationship (6) can be rewritten as:

$$\Delta\sigma_i^{S \text{ or } R} = \frac{2}{3} \left[ \sigma_{ia'd'} - \frac{1}{2}(\sigma_{ib'b'} + \sigma_{ic'c'}) \right] S_{ia'd'}^{S \text{ or } R}$$

$$+ \frac{1}{3}(\sigma_{ib'b'} - \sigma_{ic'c'}) (S_{ib'b'}^{S \text{ or } R} - S_{ic'c'}^{S \text{ or } R}) \quad (7)$$

with

$$S_{i\alpha'\alpha'}^{S \text{ or } R} = \sum_{\alpha, \beta = a, b, c} \cos\theta_{i\alpha'\alpha}^{S \text{ or } R} \cos\theta_{i\alpha'\beta}^{S \text{ or } R} S_{\alpha\beta}^{S \text{ or } R}$$

where  $\theta_{i\alpha'\alpha}$  are the angles between the principal axis system of the chemical shift tensor of a nucleus  $i$  and the molecular frame.

In eqn. (7), the quantity  $\sigma_{ia'd'} - (\sigma_{ib'b'} + \sigma_{ic'c'})/2$  corresponds to the anisotropy of the electronic shielding of atom  $i$ ,  $\sigma_i^{\text{aniso}}$ , while  $(\sigma_{ib'b'} - \sigma_{ic'c'})$  may be seen as the asymmetry of the electronic shielding,  $\sigma_i^{\text{asym}}$ . An examination of the relationship (7) shows clearly that  $\sigma_i^{\text{aniso}}$  and  $\sigma_i^{\text{asym}}$  as well as the order parameter differences ( $S_{ia'd'}^S - S_{ia'd'}^R$ ) and  $[(S_{ib'b'}^S - S_{ic'c'}^S) - (S_{ib'b'}^R - S_{ic'c'}^R)]$ , should both be large in order to detect any frequency difference,  $|\nu_i^S - \nu_i^R|$ , between the NMR signals of nucleus  $i$  for each enantiomer. Consequently, all factors which would increase either the difference in order parameters between enantiomers or the electronic shielding anisotropy of nucleus  $i$  (such as the nature of the substituents bonded to nucleus  $i$  or its hybridization state) will increase the magnitude of  $\Delta\sigma_i$ . As the magnitude of the shielding anisotropy, however, is rather small for almost all nuclei involved in classical organic molecules compared with other NMR interactions, only nuclei having the largest CSAs such as  $sp$  or  $sp^2$  carbon atoms or fluorine atoms may provide appropriate spy nuclei allowing enantiomers to be differentiated on the basis of a CSA difference.<sup>11,32,33</sup> In contrast, deuterium, proton or  $sp^3$  carbon atoms are rather poor in regard to CSA.

### Chiral discrimination using the internuclear dipolar coupling interactions

In the spectra of enantiomers dissolved in chiral liquid crystalline solutions, dipolar interactions between atoms are not averaged to zero. In this case each pair of interacting nuclei  $i$  and  $j$  for both isomers may produce a direct dipolar coupling defined in Hz as:<sup>11</sup>

$$D_{ij}^{S \text{ or } R} = -k_{ij} \left\langle \frac{S_{ij}^{S \text{ or } R}}{r_{ij}^3} \right\rangle \text{ with } k_{ij} = \frac{\mu_0}{4\pi} \frac{h\gamma_i\gamma_j}{4\pi^2} \quad (8)$$

In this equation,  $\gamma_i$  and  $\gamma_j$  are the magnetogyric ratios of nuclei  $i$  and  $j$ , and  $\mu_0$  is the permeability constant of a vacuum. The angular brackets denote an (ensemble or time) average over molecular tumbling and internal motions (vibrational motions,

conformational changes...),  $r_{ij}$  is the internuclear distance between nuclei  $i$  and  $j$  and  $S_{ij}^{S \text{ or } R}$  is the order parameter for the internuclear vector  $r_{ij}$ . Note that the magnitude of  $k_{ij}$  depends on the nuclear isotopes involved. For instance, the  $k_{ij}$  values are 7.59, 28.4, 30.19, 112.96, 120.07 kHz Å<sup>-3</sup> for <sup>13</sup>C–<sup>13</sup>C, <sup>19</sup>F–<sup>13</sup>C, <sup>1</sup>H–<sup>13</sup>C, <sup>19</sup>F–<sup>1</sup>H, <sup>1</sup>H–<sup>1</sup>H, interacting pairs, respectively.

Disregarding any discrepancies in the molecular geometry between two enantiomers, eqn. (8) shows that the chiral discrimination between enantiomers occurs when the internuclear order parameters,  $S_{ij}^{S \text{ or } R}$ , are different for the  $S$  and  $R$  isomers [Fig. 2(b)]. Although  $S_{ij}^{S \text{ or } R}$  can be related to the molecular order matrix elements,  $S_{\alpha\beta}^{S \text{ or } R}$ , using eqn. (2), it is also convenient and often easier to express this parameter relative to the  $B_0$  axis as:

$$S_{ij}^{S \text{ or } R} = \frac{1}{2} \langle 3 \cos^2 \theta_{ij}^{S \text{ or } R} - 1 \rangle \quad (9)$$

where  $\theta_{ij}^{S \text{ or } R}$  is now the angle between the internuclear vector  $r_{ij}$  and  $B_0$ . It must be emphasised that the dipolar coupling difference,  $D_{ij}^S - D_{ij}^R$ , measured from spectra varies with the relative position of the internuclear vectors  $r_{ij}^S$  and  $r_{ij}^R$  with respect to  $B_0$ . This point will be discussed in detail for the quadrupolar interaction.

Finally as underlined in the Introduction, the presence of internuclear dipolar interactions has a profound impact on the spectrum of a molecule dissolved in liquid crystals (chiral or not). As a consequence, the analysis of dipolar spectra may appear rather puzzling compared to those recorded in an isotropic medium. For instance, a first order splitting, denoted  $T_{ij}$ , observed between two coupled anisochronous nuclei  $i$  and  $j$ , is now equal to  $J_{ij} + 2\Delta T_{ij}$ , where  $J_{ij}$  is the isotropic part of the scalar coupling and  $\Delta T_{ij}$  is the anisotropic part of the total coupling that we limit to the dipolar contribution,  $D_{ij}$  [see Fig. 2(b)]. Consequently, as the sign of  $D_{ij}$  can be negative or positive, the first order splitting between two non-equivalent nuclei may be zero when  $J_{ij} = -2D_{ij}$ , producing a fortuitous decoupling. This situation is often encountered for weakly ordered liquid crystals such as organic solutions of PBLG because in this case dipolar and scalar couplings are of the same order of magnitude. Furthermore, dipolar couplings are observable between magnetically equivalent nuclei, contrary to scalar couplings. Thus, in proton liquid crystal NMR, the nuclei of an isolated methyl group produce a 1:2:1 triplet, while a methylene group produces a 1:1 doublet. In both cases the splittings are equal to  $3D_{\text{HH}}$ . Actually, in an anisotropic medium, the spectrum of any  $n$ -fully equivalent  $I = 1/2$  nuclei consists of an  $n$ -multiplet with line spacing  $3D$  and a binomial distribution of intensities.

### Chiral discrimination using the quadrupolar coupling interaction

NMR spectra of quadrupolar nuclei (spin  $I > 1/2$ ) in oriented solvents are dominated by the nuclear quadrupole–electric field gradient interaction. Disregarding spin–spin couplings, the spectrum, to first order, consists of equally spaced  $2I$  peaks corresponding to the various  $m \leftrightarrow m + 1$  transitions. The separation between the lines, denoted,  $\Delta v_{Q_i}$ , is referred to as the quadrupolar splitting as shown in Fig. 2(c). For two enantiomers oriented differently in a chiral ordered environment and assuming that the quadrupole term is much smaller than the Zeeman term, the quadrupolar Hamiltonian can be written in frequency units as:<sup>11</sup>

$$\mathcal{H}_Q^{S \text{ or } R} = \frac{1}{h} \sum_i \frac{e^2 Q_i q_{izz}^{S \text{ or } R}}{4I_i(2I_i - 1)} [3I_{zi}I_{zi} - I_i(I_i + 1)] \quad (10)$$

where  $eQ_i$  is the nuclear electric quadrupole moment of nucleus  $i$ ,  $eq_{izz}^{S \text{ or } R}$  is the component of the electric field gradient (EFG) tensor along the magnetic field ( $z$  axis) at the nucleus  $i$  for each

enantiomer. In this equation,  $eq_{izz}$ , is related to the elements of the EFG tensor in the molecular frame,  $eq_{\alpha\beta}$ , using:

$$eq_{izz}^{S \text{ or } R} = \frac{2}{3} \sum_{\alpha, \beta = a, b, c} eq_{\alpha\beta} S_{\alpha\beta}^{S \text{ or } R} \quad (11)$$

For most quadrupolar nuclei, the relaxation induced by the purely anisotropic quadrupolar interaction broadens the signals so strongly that the analytical potential produced by the DOE in a chiral mesophase is lost. However, the relaxation behaviour for some nuclei, such as boron-10 ( $I = 3$ ), boron-11 ( $I = 3/2$ ) or deuterium atoms ( $I = 1$ ), resembles that of spin-1/2 nuclei in small molecules owing to their small quadrupole moment, and produces high-resolution quadrupolar NMR spectra.<sup>13</sup> In the case of deuterons, which are monovalent atoms, the EFG is usually assumed to lie along the C–D bond direction and to be axially symmetric. Choosing one of the principal axes along the C–D bond, and safely neglecting any asymmetry parameter the quadrupolar splitting between the two lines [Fig. 2(c)] can be written as:

$$\Delta v_{Q_i}^{S \text{ or } R} = \frac{3}{2} K_{C-D_i} S_{C-D_i}^{S \text{ or } R} \quad \text{with } K_{C-D_i} = \frac{e^2 Q_D q_{C-D_i}}{h} \quad (12)$$

where  $S_{C-D_i}^{S \text{ or } R}$  is the order parameter of the C–D<sub>*i*</sub> axis for the  $R$  or  $S$  enantiomers and  $K_{C-D_i}$  is the deuterium quadrupolar coupling constant. Note that  $K_{C-D_i}$  varies depending on the hybridization state of the carbon bonded to a given deuterium. Thus  $K_{C-D_i}$  is approximately equal to  $170 \pm 5$  kHz,  $185 \pm 5$  kHz and  $210 \pm 5$  kHz, for sp<sup>3</sup>, sp<sup>2</sup> and sp carbons, respectively.<sup>11,34</sup>

Similarly to eqn. (9), the order parameter associated with the EFG for a C–D bond can be related to the molecular order parameters through eqn. (2) and is expressed relative to  $B_0$  as:

$$S_{C-D_i}^{S \text{ or } R} = \frac{1}{2} \langle 3 \cos^2 \theta_{C-D_i}^{S \text{ or } R} - 1 \rangle \quad (13)$$

As already described for the dipolar interaction, eqn. (12) shows that chiral differentiation [ $\Delta v_{Q_i}^S - \Delta v_{Q_i}^R \neq 0$ ] occurs when  $|S_{C-D_i}^S - S_{C-D_i}^R| \neq 0$ . Eqn. (13) indicates, however, that order parameters,  $S_{C-D_i}^{S \text{ or } R}$ , are composite quantities as they depend both on the angle  $\theta_{C-D_i}^{S \text{ or } R}$  and on the motional averaging ( $\langle \dots \rangle$ ). Consequently whenever two-order parameters are different between enantiomers, we generally do not know if this happens from a purely geometrical reason,  $\theta_{C-D_i}^S \neq \theta_{C-D_i}^R$ , or from a difference involving motional averaging, or both. However assuming that the motional averaging for enantiomers is more or less the same, it appears that the magnitude of the differentiation should depend strongly on the relative position of the EFG direction for both isomers with respect to  $B_0$  (Fig. 3). These variations occur because the trigonometric function,  $(3\cos^2\theta - 1)/2$ , is very steep for angles around the magic angle,  $\theta_m = 54.7^\circ$  (for which the function is null, and hence  $S_{C-D_i}^{S \text{ or } R} = 0$ ), and rather flat in the angular ranges of  $[-5, +5^\circ]$  and  $[+85, +95^\circ]$ . Analyzing the evolution of the calculated quadrupolar splitting difference, assuming  $\theta_{C-D_i}^S = \theta_{C-D_i}^R + 10^\circ$ , and the corresponding spectra plotted in Fig. 3, we can easily see that larger chiral discriminations are obtained when  $\theta_{ij}^S$  and  $\theta_{ij}^R$  vary in the interval  $\theta_m \pm 20^\circ$ . This range of angles corresponds also to the smallest values for  $S_{C-D_i}^{S \text{ or } R}$  and subsequently to the smallest magnitudes of quadrupolar splittings. As shown in Fig. 3, there exist several particular spectral situations corresponding to either the cancellation of quadrupolar splitting for one of the enantiomers ( $\theta_{ij}^S = \theta_m$  or  $\theta_{ij}^R = \theta_m$ ) or the disappearance of the chiral discrimination ( $S_{ij}^S = S_{ij}^R$ ). Note that the various spectral situations simulated here in the case of spins-1 could be also observed for two dipolar coupled magnetically equivalent spins-1/2. The great efficiency of deuterium NMR in the discrimination of enantiomers in PBLG mainly originates from the relatively large magnitude of the deuterium quadrupolar coupling constants,  $K_{C-D}$ , compared with almost all  $k_{ij}$ ,

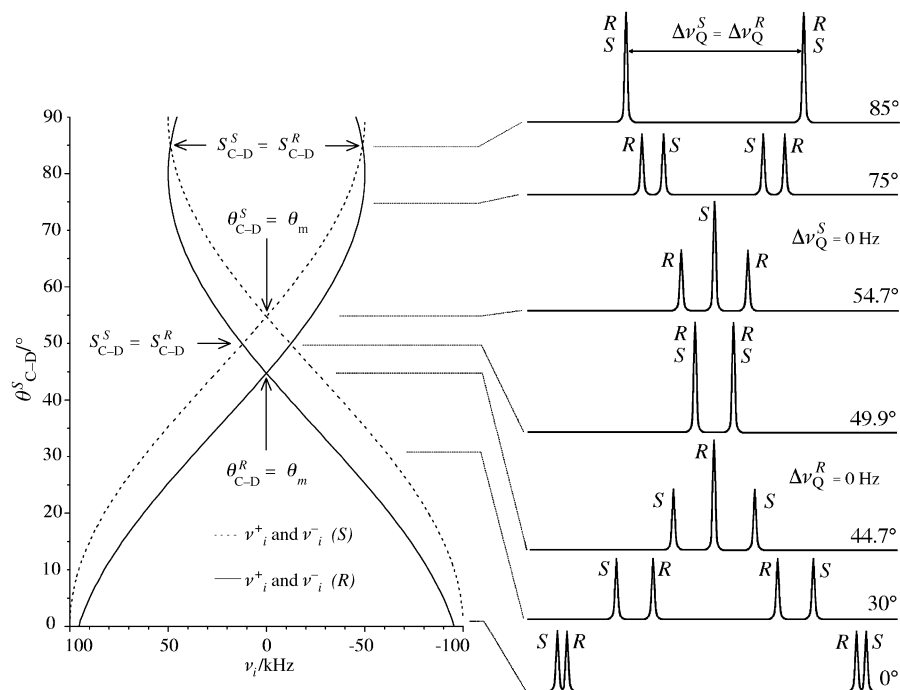


**Fig. 3** Theoretical evolution of the two components ( $\nu_i^-$  and  $\nu_i^+$ ) of a quadrupolar doublet associated with two enantiomers, versus the angle  $\theta_{C-D}^S$ . We have assumed that  $K_{C-D} = 133$  kHz and the difference  $\theta_{C-D}^S - \theta_{C-D}^R = +10^\circ$  for all values. On the right of the figure, the expected spectra for various angles  $\theta_j$  are shown. Note the four particular situations corresponding to  $\theta_{C-D}^R = \theta_m$ ,  $S_{C-D}^S = S_{C-D}^R$  when  $\theta_{C-D}^S < \theta_m$ ,  $\theta_{C-D}^S = \theta_m$  and  $S_{C-D}^S = S_{C-D}^R$  when  $\theta_{C-D}^S > \theta_m$ , respectively. The S and R assignment given for the initial spectrum is arbitrary.

involved in the dipolar interaction. Indeed, even when the DOE between two enantiomers is rather small, the magnitude of the deuterium quadrupolar coupling constant for a C–D bond can make the difference in their residual quadrupolar splittings,  $|\Delta\nu_{Q_i}^S - \Delta\nu_{Q_i}^R|$ , measurable.

### Experimental and NMR technical considerations

In this technique, PBLG sample preparation is very important because it may affect strongly the quality of NMR spectra, in particular the linewidths. The typical procedure to prepare a PBLG sample consists of directly weighing 2–100 mg of racemic material, 80–100 mg of PBLG and adding about 350–500 mg of co-solvent into a 5 mm NMR tube. Note that the viscosity of the mixture and the evaporation of the co-solvent preclude the possibility of preparing and handling the sample outside the NMR tube. Under these conditions, the total volume of the sample is optimal compared to the length of the coil of a 5 mm diameter dual probe-head. In this study we have added 100 mg of PBLG (DP = 562, MW  $\approx$  120 000), 100 mg of 1-chloropropan-2-ol (CP) in racemic mixture and 350 mg of dry chloroform. The polymer was purchased from Sigma and used with no further purification, however numerous preparative methods of PBLG are possible and have been described in the literature.<sup>24,35–37</sup> It is recommended to wait for slow dissolution of the compounds in the NMR tube (which was sealed to prevent any co-solvent evaporation) and then to centrifuge the sample in both directions until an optically homogeneous birefringent phase is obtained. Finally, before measuring the NMR spectra, the sample was kept for about 15 min in the magnetic field in order to achieve a good thermal equilibration and the complete unwinding of the cholesteric pitch prior to starting the shimming procedure.

NMR experiments in PBLG can be performed on any routine spectrometer and no special hardware equipment is required. Nevertheless, using a high magnetic field is a strong advantage to increase the chemical shift dispersion and to record low sensitivity nuclei at natural abundance level such as deuterium. In this work, all NMR spectra were obtained on a Bruker DRX-400 high-resolution NMR spectrometer equipped with an

inverse 5 mm multinuclear probe, the operating frequencies being 400.1, 100.6 and 61.4 MHz for  $^1\text{H}$ ,  $^{13}\text{C}$  and  $^2\text{H}$ , respectively. The NMR probehead was tuned and matched very carefully to minimize losses in probe efficiency. This is of importance for detecting nuclei of very low natural isotopic abundance such as deuterons. The NMR tube was not spun in the magnet and the temperature of the sample was regulated carefully at  $298.0 \pm 0.1$  K by the Bruker BVT 3000 temperature unit in order to prevent substantial temperature fluctuations. Note here that the sample rotation does not produce a significant improvement in the spectral resolution when the magnetic field homogeneity is good whereas a good long term thermal stability ensures an optimal spectral resolution. The field-frequency lock was not used, but the field drift of our magnet is small enough to allow for a long time accumulation without significant line broadening. When long term field stability is poor, field-frequency lock on a deuterium signal is possible, one component of the quadrupolar doublet of the deuterated solvent providing the lock signal for instance. The recording of natural abundance deuterium spectra of solutes is, however, not possible in this case. One solution consists of using a fluorine-19 signal as lock signal. Thus a few drops of  $\text{CFCl}_3$  can be added to the co-solvent without perturbing the PBLG phase, but this technical solution requires a fluorine-19 lock device and a suitable probe. In order to avoid possible sample heating which can produce some line broadening, proton-decoupled carbon or deuterium spectra are recorded applying broadband proton decoupling using the WALTZ-16 composite pulse sequence ( $\approx 0.5$  W of rf power).<sup>38</sup> Note here that the proton decoupling in PBLG does not necessitate more power than for isotropic samples because of the rather small amplitude of the residual heteronuclear dipolar interactions. Other specific experimental details for each technique will be given in the figure captions.

### Description and analysis of various anisotropic NMR tools in PBLG

#### Proton NMR spectroscopy

Proton spectra of oriented molecules in classical thermotropic LCs are dominated by the residual dipolar couplings and yield

usually non-trivial second order spectra. The reason for this is that the magnitude of partially averaged  $^1\text{H}$ - $^1\text{H}$  dipolar couplings are often much larger than the chemical shift differences.<sup>11</sup> Actually, this analytical circumstance is less often encountered using organic solutions of PBLG because of the weak degree of molecular orientation in PBLG. The value of order parameters are in the range  $10^{-3}$  to  $10^{-5}$ , and consequently the dipolar couplings are often small (negative or positive) values compared to Larmor frequency differences.<sup>9,10</sup> Consequently, the analysis of proton spectra in PBLG may often be carried out at first order and allows detection of a possible chiral discrimination.

To illustrate our purpose, Fig. 4 shows the proton signals of the methyl group in ( $\pm$ )-CP where two different spectral

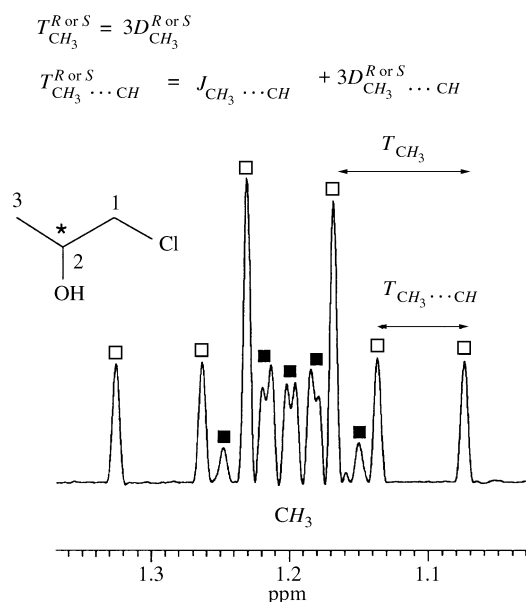


**Fig. 4** Proton signal of the methyl group of ( $\pm$ )-CP. The spectrum was Fourier transformed after adding 256 scans. The peaks due to each enantiomer are labelled by (□) and (■). Zero filling, digital gaussian filtering (GB = 40% and LB = -9 Hz) and a baseline correction were applied to increase the digital resolution and enhance the spectral aspect.

patterns, centred on the same chemical shift, may be observed, one for each enantiomer. As already suggested in the theoretical section, this situation illustrates perfectly that the very weak sensitivity of proton CSA toward the DOE does not generally allow a chemical shift difference between enantiomers to be measured on the  $^1\text{H}$  spectra (even at 400 MHz). In contrast, the superposition of two spectral patterns for the methyl shows the chiral separation of enantiomers through a difference in the residual  $^1\text{H}$ - $^1\text{H}$  dipolar couplings. Thus, for one of the enantiomers (labelled using white squares) we obtain a doublet of triplets due to the dipolar couplings between the three equivalent protons of the methyl group and to the coupling with the proton directly attached to the asymmetric carbon. From the values  $T_{\text{CH}_3}$  and  $T_{\text{CH}_3\cdots\text{CH}}$ , measured directly from the spectrum, we can determine the  $^1\text{H}$ - $^1\text{H}$  residual dipolar constants. We find here  $|D_{\text{CH}_3}| = 12.4$  Hz and  $|D_{\text{CH}_3\cdots\text{CH}}| = 9.1$  Hz. The spectral pattern associated to methyl group of the other enantiomer (labelled using black squares) is more complicated than the first because the dipolar couplings between the protons of  $\text{CH}_3$  and the diastereotopic protons of the  $\text{CH}_2$  group are not averaged to zero as previously. This perfectly emphasises the variation of dipolar couplings between the *S* and the *R* isomers and shows the influence of the DOE on the spectral analysis in chiral liquid crystals. However as the order parameters and subsequently the  $D_{ij}$  values are temperature-sensitive, we can modify the spectral patterns by changing the sample temperature and, hopefully, simplify the analysis. The determination of all dipolar couplings is not trivial and requires the use of spectral simulation

programs such as PANIC.<sup>39</sup> For the *R* enantiomer of CP, we have measured  $|D_{\text{CH}_3}| = 4.2$  Hz,  $|D_{\text{CH}_3\cdots\text{CH}}| = 3.2$  Hz and  $|D_{\text{CH}_3\cdots\text{CH}_2}| = 3.3$  Hz. Finally, it is noteworthy that the chiral discrimination may also be seen on the NMR signal of the methylene and methine groups through  $^1\text{H}$ - $^1\text{H}$  dipolar coupling differences, but they are not shown here.

Although chiral differentiation was visualized in this example using  $^1\text{H}$  NMR, it is clear that when the number of interacting protons in the molecules becomes larger, the analysis of the  $^1\text{H}$  spectra becomes very difficult. In this case, the chiral discrimination between enantiomers cannot always be unambiguously established because doubling of peaks may arise, for instance, from the long distance dipolar couplings. Two solutions can be suggested to check if a chiral discrimination occurs or not. First, it is always convenient to apply a selective decoupling of protons which are susceptible to interact with the signal suspected to give a chiral discrimination. When doubt still arises, the spectra in a racemic mixture of PBLG and its enantiomer, PBDG, dissolved in  $\text{CHCl}_3$  may then be recorded.<sup>22,31</sup> Indeed in such a mixture, the fast exchange between chiral solutes and the vicinity of PBLG and PBDG eliminates the chiral discrimination, and hence results in a significant simplification of spectra, which can give valuable information with regard to chiral discrimination.<sup>31</sup> This latter solution can be also successfully applied using the other NMR spectroscopies described below such as carbon-13 or deuterium NMR. However in proton NMR, these alternatives will remain limited for large, chiral molecules because the numerous long distance dipolar couplings together with the superposition of the  $^1\text{H}$  spectra for each enantiomer can yield either significant line broadening of the resonances or an excessive peak overlap which totally prevents their analysis. We reach, then, the limits of the applicability of the proton NMR spectroscopy in PBLG solvent. In such cases, carbon-13 NMR spectroscopy can offer a first and reliable alternative.

### Carbon-13 NMR spectroscopy in natural abundance

In spite of the lower natural isotopic abundance of carbon-13 atoms, the advantages of using carbon-13 NMR in PBLG are obvious compared with proton NMR.<sup>5,32</sup> In the first place, the spectral analysis of rare spins in anisotropic medium is considerably simplified due to the absence of coupling between two dilute spins. Second, the magnetic fields used in routine NMR are sufficiently strong to reach a satisfying *S/N* ratio with a relatively small amount of material and short experimental times. Moreover because of its high molecular weight and liquid crystalline nature, the broad carbon-13 NMR resonances arising from PBLG do not interfere with the analysis of the solute signals. Consequently in a second approach, we have demonstrated that natural abundance carbon-13 NMR may be successfully applied to visualize enantiomeric discrimination, through a difference of  $^{13}\text{C}$ - $^1\text{H}$  dipolar interactions and/or C-13 chemical shift anisotropies when proton NMR gives rather poor or unconvincing results.<sup>5</sup>

**1D proton-coupled carbon-13 experiments.** Fig. 5(a), shows the proton-coupled carbon-13 signal of the methyl group of ( $\pm$ )-CP. Here again, we distinguish two spectral patterns, namely a doublet of quartets for each enantiomer, clearly indicating chiral differentiation. To check this analysis, we have recorded the carbon-13 signal of the methyl carbon applying a selective decoupling of the proton attached on the asymmetric carbon. In this case, we eliminate the dipolar splitting,  $T_{\text{CH}_3\cdots\text{H}}$ , and we observe only two distinct quartets, corroborating unambiguously the discrimination of enantiomers. Note that recording the proton-coupled carbon-13 signal of the methyl in a racemic mixture of PBLG and PBDG would give a single dedoubled quartet, showing that chiral discrimination occurred in the PBLG phase. From the values of  $nT_{\text{CH}}$  ( $n$  is the number of

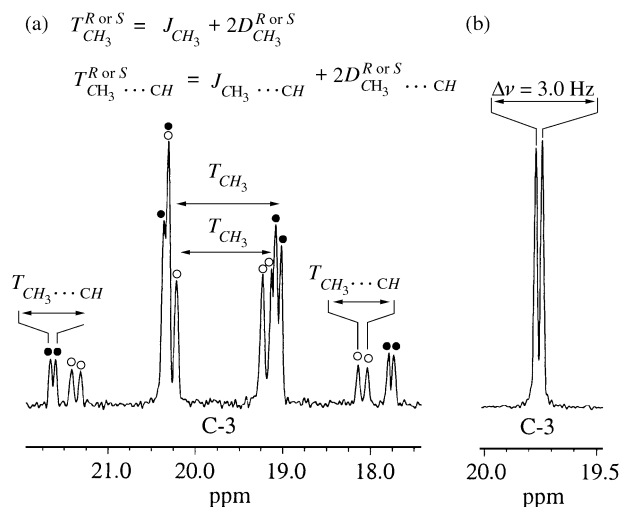


**Fig. 5** (a) Carbon-13 and (b)  $^{13}\text{C}\{-^1\text{H}\}$  signal of the methyl group of ( $\pm$ )-CP. The spectra were obtained after adding 2000 and 1000 scans of 16 K data points, respectively. The recycling delay was 2 s. For spectrum (a), proton decoupling was applied during the relaxation delay period in order to gain a nuclear Overhauser effect. The peaks arising from each enantiomer are labelled (○) and (●).

bonds separating the two coupled nuclei in the molecular skeleton), measured directly from the spectrum, we can calculate the residual dipolar coupling constants,  $^nD_{\text{CH}}$ . As the sign of  $^1J_{\text{CH}}$  and  $^3J_{\text{CH}}$  are known to be positive<sup>33</sup> and considering that  $^1J_{\text{CH}}$  and  $^3J_{\text{CH}}$  are larger than  $^1D_{\text{CH}}$  and  $^3D_{\text{CH}}$ , in the PBLG phase,<sup>9,10</sup> we are able to determine the absolute sign of those dipolar couplings. In contrast, the sign of  $^2J_{\text{CH}}$  can be positive or negative, consequently the sign of  $^2D_{\text{CH}}$  cannot be ascertained directly. In this example, the four corresponding residual dipolar couplings derived from the spectrum analysis are  $D_{\text{CH}_3} = -8.5$  Hz and  $D_{\text{CH}_3\cdots\text{CH}} = +3.8$  Hz (○) and  $D_{\text{CH}_3} = +1.5$  Hz and  $D_{\text{CH}_3\cdots\text{CH}} = +1.7$  Hz (●) assuming that  $J_{\text{CH}_3\cdots\text{CH}}$  and  $T_{\text{CH}_3\cdots\text{CH}}$  are positive. Note here that at 298 K, we are not able to measure the dipolar couplings between the methyl group and the diastereotopic protons on the methylene group. Disregarding the fortuitous elimination of dipolar splittings ( $J + 2D = 0$  Hz) and lack of spectral resolution, we may assume that the large internuclear distance ( $r_{\text{CH}_3\cdots\text{CH}_2} > 2.8$  Å) and the small magnitude of order parameters in PBLG give a negligible dipolar interaction between those protons and the methyl carbon. Consequently no further splittings are visible in the spectral pattern. We can also remark that the spectral patterns are not perfectly centered on the same chemical shift owing to a small but measurable difference of carbon-13 CSA. As we will see in the next section, this small difference is more clearly visible on the proton-decoupled carbon-13 spectrum. Finally it can be stated that a chiral discrimination has also been detected on the other two carbons on the basis of a difference in dipolar couplings, but they are not presented here.

In this example, we were able to clearly visualize a chiral discrimination based on a difference of  $^{13}\text{C}\{-^1\text{H}\}$  residual dipolar couplings. It is clear, however, that such well-resolved spectra will not always be obtained when the molecule under study possesses a large number of interacting nuclei. Actually for medium to large sized molecules, we may reach again the limits of the applicability of the proton-coupled carbon-13 NMR similar to the situation which is encountered in overcrowded proton NMR spectra. For chiral compounds exhibiting an isolated group (such as a methyl group) far removed from other protons in the molecule, it may be convenient to record the proton-coupled carbon-13 spectrum in order to detect the separation of enantiomers through a difference in the  $^{13}\text{C}\{-^1\text{H}\}$  dipolar couplings. When proton-coupled carbon-13 spectra cannot be conveniently resolved it becomes necessary to cancel out all dipolar interactions. By recording the proton-decoupled carbon-13 spectrum, we can, therefore, expect to distinguish

between enantiomers through a difference in their carbon-13 CSA.

**1D proton-decoupled carbon-13 experiments.** The major advantage of proton-decoupled carbon-13 NMR ( $^{13}\text{C}\{-^1\text{H}\}$ ) in PBLG is the simplicity of the spectral analysis. First, with broadband proton decoupling, carbon-13 spectra of solutes usually show resolved peaks which can be assigned to all non-equivalent individual carbon atoms in the molecule, similar to that for an isotropic sample. When the difference in C-13 chemical shift anisotropy between the *S* and *R* isomers for a given carbon *i* is large enough, then we observe two distinct resonance lines located at  $\nu_i^S$  and  $\nu_i^R$  as depicted in Fig. 2(a). Second, as the carbon-13 CSAs are rather small in PBLG, the chemical shifts of each carbon are very close to those observed in the isotropic solvent. Consequently the assignment of the C-13 resonances in PBLG is often trivial and comparison with the isotropic spectrum readily reveals the carbons of the chiral molecule which are discriminated.

Although the carbon-13 chemical shift anisotropies are much greater than for the proton, the chemical shift differences measured in almost all spectra are typically just a few Hz (typically 3–15 Hz), except for some sp carbon atoms for which chiral discriminations of up to 40 Hz have already been measured.<sup>5</sup> Nevertheless these small differences allow the visualization and the measurement of enantiomeric excess using classical numerical integration or iterative curve-fitting. As for overcrowded  $^1\text{H}$  and  $^{13}\text{C}$  spectra, it is clear that a good homogeneity of both sample and magnetic field is required to reach an optimal enantiomeric discrimination. Under the experimental conditions described above, the linewidths at half-height commonly observed in  $^{13}\text{C}\{-^1\text{H}\}$  spectra are *ca.* 2–4 Hz. Note that when this spectral resolution is not reached, it can be useful to slightly increase the sample temperature. Indeed a greater fluidity of the phase may give an important improvement in the spectral resolution. When no significant effect is obtained, it is recommended to heat the sample for a few hours prior to centrifuging the sample in both directions again. In fact this latter procedure can produce a more homogenous distribution of each component in the mixture, thus avoiding possible concentration gradients in the sample.

Finally, compared with proton-coupled carbon-13 NMR,  $^{13}\text{C}\{-^1\text{H}\}$  NMR offers an important advantage in terms of sensitivity and *S/N* ratio, since all signals are concentrated in only one resonance for each carbon. This situation enhances considerably the quantitative aspects of this approach through the greater precision that can be reached in measuring the *ee* values. Usually a sufficient *S/N* ratio is obtained after an experimental time varying between 1 and 5 h depending on the available amount of solute and its molecular weight. The experimental enantiomeric excess determined on such spectra by integration can be within 2% of the true value.<sup>6</sup> Generally, we estimate that the accuracy on the enantiomeric excess measurements is about 5% of the true value when the spectrum is recorded and processed using standard conditions.<sup>40,41</sup>

Fig. 5(b), shows a small but visible chiral discrimination ( $|\nu_i^S - \nu_i^R| = 3$  Hz) on the signal of the methyl group for ( $\pm$ )-CP. Although the probability for detecting a chiral discrimination is generally greater for carbons having an sp and sp<sup>2</sup> hybridization state, the discrimination on sp<sup>3</sup> carbons is also possible as seen in this example. However, we must note that none of the carbons bonded to the heteroatoms in the molecule displays a line separation. The result is rather surprising if we consider that the strength of the carbon-13 CSA increases with the electronegativity of the substituents.<sup>33</sup> However, as already emphasised in the theoretical section, the electronic shielding anisotropy and the asymmetry term are not the only parameters involved in the chiral discrimination, and the order parameter differences ( $S_{ia'a'}^S - S_{ia'a'}^R$ ) and  $[(S_{ib'b'}^S - S_{ic'c'}^S) - (S_{ib'b'}^R - S_{ic'c'}^R)]$ ,

may have a large effect on the frequency difference of both isomers for a given carbon. In this particular example, we may suppose that the angle,  $\theta$ , between the magnetic field and one of the principal axes of the CSA tensor for the methylene and methine carbon are located in the region where the function  $(3\cos^2\theta - 1)/2$  is rather flat and produces a negligible DOE, thus leading to absence of chiral discrimination.

In contrast with the homo- and hetero-nuclear spin-spin coupling interactions that are independent of magnetic field magnitude, eqn. (4) shows that the sensitivity of CSA to the DOE increases with  $B_0$ . Consequently, the use of NMR spectrometers operating at higher magnetic fields enhances considerably the possibility to detect enantiomeric discriminations on all non-equivalent carbons of the chiral molecule. Thus, when recording the  $^{13}\text{C}\{-^1\text{H}\}$  spectra of ( $\pm$ )-CP at 201.2 MHz (18.4 T), the chemical shift difference of 3.0 Hz measured for the methyl carbon would become around 6 Hz under the same experimental conditions. Such a difference would offer a very comfortable separation between these signals which are associated with an  $\text{sp}^3$  carbon. In addition, we may expect to observe a chemical shift difference for the two other carbon signals of the molecule, thus increasing the probability to detect a chiral discrimination.

**2D  $^{13}\text{C}\text{-}^{13}\text{C}$  INADEQUATE experiments.** The detection of coupled dilute spin systems such as two carbon-13 nuclei in a CLC solvent is not trivial to achieve for three reasons. First, the probability for observing chiral isotopomers possessing two carbon-13 nuclei is only 1/10000 and the intensity of the corresponding resonances will be a factor 200 lower than the intensity of signals from the isolated carbon-13 nuclei. Second, the  $k_{\text{CC}}$  parameter for two interacting carbon-13 nuclei is small ( $\gamma_{\text{C}}\gamma_{\text{C}}/\gamma_{\text{C}}\gamma_{\text{H}} \approx 0.25$ ) and the larger internuclear distances between adjacent carbon-13 atoms (1.20–1.54 Å *cf.* 1.09 Å for a  $^{13}\text{C}\text{-}^1\text{H}$  bond) significantly reduces the sensitivity of  $^{13}\text{C}\text{-}^{13}\text{C}$  dipolar interaction to the DOE compared with that of the  $^{13}\text{C}\text{-}^1\text{H}$  dipolar interaction. Finally the detection of two coupled carbon-13 spins is not simple, and hence requires usually the creation of double quantum coherences using the well-known 2D INADEQUATE experiment, the basic pulse sequence of which is shown in Fig. 6(a).<sup>42–44</sup> The condition for optimum transfer of one quantum into double-quantum coherence is satisfied with the delay  $\tau = (2n + 1)/(4T_{\text{CC}})$  where  $n$  is an integer, and consequently the choice of the  $\tau$  value is important. In the PBLG phase, the very small magnitude of one-bond  $^{13}\text{C}\text{-}^{13}\text{C}$  dipolar couplings (a few Hz) compared with the range of one-bond  $^{13}\text{C}\text{-}^{13}\text{C}$  scalar couplings (20–200 Hz, depending on hybridization state of coupled carbons)<sup>33</sup> allows the assumption that  $1T_{\text{CC}} \approx {}^1J_{\text{CC}}$ . Consequently, despite the fact that the exact values of  $1D_{\text{CC}}$  are unknown, the loss of signal during the single-to-double quantum transfer, due to a non-ideal value of  $\tau$  is weak and the detection of double quantum remains possible. Note here that the magnitude of long-distance  $^{13}\text{C}\text{-}^{13}\text{C}$  dipolar couplings is generally too small to be experimentally detected. Finally the  $\alpha$  read pulse ( $\alpha = 90, 120$  or  $135^\circ$ ) depends on the phase cycling employed and allows either optimization of the double quantum coherence or suppression of the quadrature images in the  $F_1$  dimension.<sup>43,45</sup>

Related to such 2D experiments, Levitt and coworkers were the first to report the measurements of  $^{13}\text{C}\text{-}^{13}\text{C}$  dipolar couplings of liquid crystalline molecules using the 2D INADEQUATE sequence.<sup>46</sup> In our case, the low concentration of chiral solutes in the PBLG phase reduces further the sensitivity of this experiment, thus raising another difficulty. In other words, the visualization of enantiomeric discrimination based on a difference of  $^{13}\text{C}\text{-}^{13}\text{C}$  dipolar couplings is a difficult but challenging task.

Fig. 6(b) displays part of the 2D INADEQUATE experiment of ( $\pm$ )-CP recorded in PBLG after 15 h of experimental time

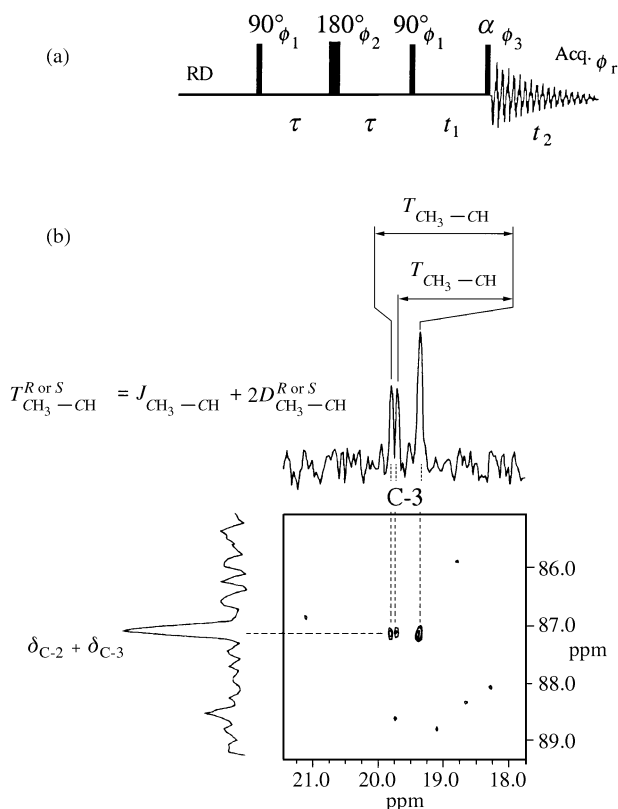


**Fig. 6** (a) Basic INADEQUATE pulse scheme for carbon-13 2D NMR spectroscopy. (b) 100.6 MHz INADEQUATE 2D spectrum of ( $\pm$ )-CP in PBLG. The spectrum was recorded with data matrix of 384 ( $t_1$ )  $\times$  2048 ( $t_2$ ) data points. The recycle delay and the preparation time  $\tau$  were set to 2 s and 6.3 ms, respectively. The number of free induction decays added for each  $t_1$  increment was 256. No apodization was applied. The 2D contour plot is presented in magnitude mode.

(overnight). As in an isotropic solvent, all dipolar coupled two-spin systems straddle the skew diagonal of slope 2, each being located at the sum of their Larmor frequency,  $\nu_i + \nu_j$ , in the  $F_1$  double-quantum dimension. Two slices parallel to the  $\omega_2$  axis were observed in the 2D contour plot and permit the unambiguous identification of each  $^{13}\text{C}\text{-}^{13}\text{C}$  doublet, and assignment of each of them on the basis of chemical shifts. On the 2D contour plot, we can observe two partially overlapping dipolar doublets associated with the carbon-13 atom of the methyl group, thus showing two different  $^{13}\text{C}\text{-}^{13}\text{C}$  dipolar couplings between the C-2 and C-3 carbons, one for each enantiomer. This situation occurs when the two dipolar doublets are not centered on the same chemical shift due to a CSA difference between enantiomers (here *ca.* 3 Hz). This part of the 2D spectrum unambiguously evidences chiral discrimination. This result was also confirmed by recording the 2D INADEQUATE spectrum of ( $\pm$ )-CP in the isotropic state at 298 K because in this instance, only a single doublet was detected between this pair of adjacent carbons. The residual dipolar constant  $D_{\text{CH}_3\text{-CH}}$  measured on the 2D spectrum is +2.6 and  $-1.1$  Hz for one enantiomer and the other, the scalar coupling measured in isotropic solution,  $J_{\text{CH}_3\text{-CH}}$ , between the two components being equal to +38.9 Hz ( $1J_{\text{CC}}$  is always positive).

It is of note that this is the first enantiomeric discrimination of a chiral molecule using  $^{13}\text{C}\text{-}^{13}\text{C}$  dipolar interaction since no successful results using this NMR technique have, up to now, been recorded. Even though the natural sensitivity of the 2D INADEQUATE experiment is rather poor, this result establishes that enantiomeric discrimination based on a difference of  $^{13}\text{C}\text{-}^{13}\text{C}$  dipolar coupling is possible and should not be neglected. However, it is clear that the analytical potential of this tool is rather limited because the condition for optimum transfer into double-quantum coherence substantially restricts its

use for accurate quantitative measurements of enantiomeric excess.

### Deuterium NMR spectroscopy in natural abundance

As already mentioned in the theoretical section, the deuterium quadrupolar interaction is the most sensitive interaction to the DOE of enantiomers. Consequently, in the earliest studies, we have focused on chiral discrimination using labelled materials.<sup>14,47</sup> Among successful results already reported, the great sensitivity of this approach allowed us to visualize the chirality of almost all investigated chiral molecules.<sup>4,5,48,49</sup> Among the compounds known to be very difficult to analyse, but showing a chiral discrimination in PBLG, are ethers, monohalogenated hydrocarbons and non-functionalised cycloalkenes.<sup>4</sup> Also we have reported the discrimination of molecules that are chiral by virtue of isotopic substitution.<sup>3</sup> Although synthetic methods for selectively introducing deuterium in chiral molecules are numerous and well documented, it is clear that this is not always possible or easy to do, and may be time-consuming.<sup>4,5</sup> Consequently, isotopic labelling may be a serious limitation to this investigation technique.

To eliminate the synthetic step, we have recently demonstrated that isotopic enrichment of chiral solutes was not necessary to yield observable deuterium resonances in PBLG, despite its very low sensitivity ( $1.45 \times 10^{-6}$  with respect to proton).<sup>16</sup> Actually, calculations indicate that NAD-NMR experiments have sensitivities comparable with those of the above 2D INADEQUATE experiments. However for the same experimental time, NAD-NMR experiments are more advantageous in terms of *S/N* ratio because the deuterium  $T_1$  relaxation values of solutes dissolved in PBLG ( $\approx 0.8$ – $1$  s) are generally much shorter than the  $T_1$  values of carbon-13, allowing a faster repetition rate of the pulsing. Consequently, enantiomeric differentiation of chiral compounds using natural abundance deuterium (NAD) NMR is perfectly possible using standard NMR equipments, and provides, therefore, a second and interesting alternative to other previous techniques.<sup>6,16,50</sup>

Assuming that the detection of a rare spin such as deuterium in natural abundance is not an insurmountable obstacle in terms of signal sensitivity, site-specific labelling of the molecules would, therefore, not be required. Furthermore, it would permit the simultaneous probing of all possible deuterated sites of the molecule, thus increasing the probability to visualize a chiral differentiation between enantiomers. At natural abundance level,  $^2\text{H}$ – $^2\text{H}$  spin–spin couplings are not detected (owing to the very low probability of observing two interacting deuterons in the same isotopomer). Consequently, as all the couplings with protons are eliminated through decoupling, the natural abundance  $^2\text{H}$ – $\{^1\text{H}\}$  spectra in organic solutions of PBLG consist of the superposition of independent quadrupolar doublets corresponding to all non-equivalent deuterons in each of the enantiomers.<sup>6,16,50</sup> Thus, disregarding the doublets originating from organic co-solvent, we can expect  $2n$  doublets ( $4n$  peaks) to be observed in the NAD spectrum for a racemic mixture of enantiomers possessing  $n$  non-equivalent deuterons, assuming that all deuterated chiral isotopomers are discriminated and neither line overlaps nor null quadrupolar splittings occur. This evaluation can be, however, reduced to  $2n - 1$  doublets for molecules possessing an –OD or –ND group, since no chiral discrimination has (until now) been detected for such groups, owing to the fast exchange of their deuteron. In the case of ( $\pm$ )-CP and disregarding solvent quadrupolar doublets (one doublet for  $\text{CDCl}_3$ ), eight different chiral isotopomers exist in the mixture and a maximum of eight quadrupolar doublets are expected to be detected if all deuterated sites show chiral differentiation. This is because ( $\pm$ )-CP contains two diastereotopic nuclei associated with deuterons of the methylene group. For this group, four quadrupolar doublets corresponding to the (*S*, pro-*S*), (*S*, pro-*R*), (*R*, pro-*S*), (*R*, pro-*R*) deuterons of

the *S* and *R* isomers can be expected to be seen in the NAD-NMR spectrum (when all isomers are discriminated and without peak overlapping). Traditionally we use the term ‘*semi-isotopic*’ diastereoisomers for all deuterated isotopomers bearing a classical asymmetric carbon and an asymmetric carbon by virtue of isotopic substitution.

It must be clear that for larger molecules, the correlation between the two components for each quadrupolar doublet will not always be simple to achieve, mainly due to overlapping of peaks, and will require the use of proton-decoupled deuterium 2D-NMR experiments.<sup>6,50,51</sup> Consequently, we have developed several two-dimensional autocorrelation deuterium NMR experiments referred to as QUOSY (for QUadrupole Ordered Spectroscopy), which facilitate the analysis of overcrowded NAD spectra. Among them, the Q-COSY and Q-resolved experiments and their composite pulse variants were found to be the most useful 2D sequences for applications in NAD-NMR or when the problem of sensitivity is crucial (very low degree of deuteration). The optimised sequences using pulse composites and the corresponding full phase cycling are described in refs. 6 and 51.

Fig. 7 shows the 2D NAD Q-COSY spectrum of ( $\pm$ )-CP recorded over 14 h (overnight) with digital filtering and oversampling in order to enhance the dynamic range of the analogue-to-digital converter (ADC).<sup>52,53</sup> The 2D contour plot is symmetrized prior to the tilt procedure and is displayed in

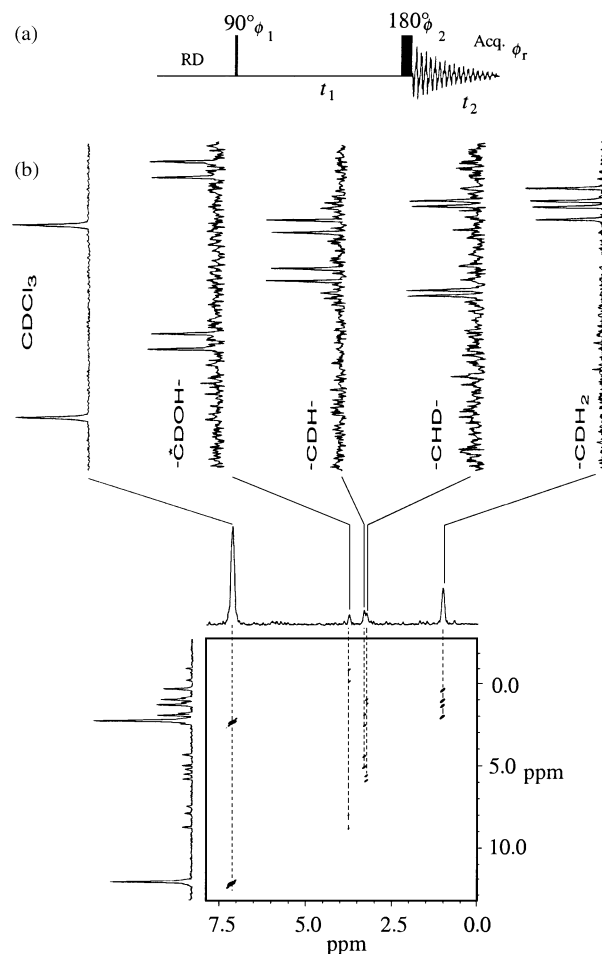


**Fig. 7** (a) Basic Q-COSY pulse scheme for deuterium 2D NMR spectroscopy in partially ordered solvents. (b) 61.4 MHz tilted NAD Q-COSY 2D spectrum of the ( $\pm$ )-CP in PBLG and slices parallel to the  $\omega_1$  axis corresponding to the deuterium spectrum of each monodeuterated isotopomer in the mixture. The number of free induction decays added for each  $t_1$  increment is 384. The recycling delay was 0.5 s and the spectral width in both dimensions was 2500 Hz. The data matrix of 300 ( $t_1$ )  $\times$  1400 ( $t_2$ ) was weighted with a gaussian window ( $\text{GB}_1 = 50\%$ ,  $\text{LB}_1 = -2.0$  Hz and  $\text{GB}_2 = 45\%$ ,  $\text{LB}_2 = -1.5$  Hz) in  $t_1$  and  $t_2$  dimensions, respectively, and zero-filled to 512 ( $t_1$ )  $\times$  2048 ( $t_2$ ) prior to 2D FT.

magnitude mode in order to cancel out the phase-twist lineshapes.<sup>6</sup> In this 2D spectrum, the chemical shift of each non-equivalent deuteron appears in the  $F_2$  dimension. From each of them, we can observe the deuterium signals of the corresponding isotopomers in the mixture, the most unshielded trace (7.3 ppm) being the chloroform quadrupolar doublet. The analysis of each slice indicates that all deuterons in the molecule exhibit two quadrupolar doublets, one for each enantiomer. In particular the two diastereotopic deuterons of the methylene group distinctly show two pairs of quadrupolar doublets which are not centered on the same chemical shift. Strong differences of  $S/N$  ratio for each extracted slice are observed. This situation reflects that the number of equivalent deuterons (magnetic equivalence) for the various possible isotopomers is different. Thus, the signals associated with the deuteron attached to the asymmetric carbon are three times smaller than the signal of the methyl group, and hence the strong reduction of  $S/N$  ratio observed on the corresponding trace. The precision of the enantiomeric measurement for ( $\pm$ )-CP was not investigated here, but previous results have shown that such determination is possible within an accuracy of *ca.* 10% for reasonable  $S/N$  ratio, thus already giving a valuable estimation of the enantiomeric excess.<sup>6</sup>

Finally it should be noted that chloroform is the most efficient solvent for NAD NMR in PBLG. Apart from the fact that it dissolves a wide range of organic compounds, the linewidths at half-height of solutes measured on the  $^2\text{H}\{-^1\text{H}\}$  spectra are usually low (2–8 Hz). Second, this solvent contains a single deuterated isotopomer giving rise only to a single additional quadrupolar doublet in the NAD spectrum. Third, the number of deuterons per unit volume is not excessively large relative to those of the chiral solutes, thus minimizing the digitization problems associated with the dynamic range of the ADC. Fourth, the deuterium signal of chloroform can be used as an internal reference for the NAD spectra.

With this last analytical approach, we show that the enantiomeric discrimination of ( $\pm$ )-CP in 2D NAD-NMR using a 9.4 T field and standard NMR equipment is possible. These present results confirm the feasibility, potential and usefulness of NAD NMR spectroscopy, thus providing a further practical solution to DOE measurements in PBLG without site-specific isotopic labelling. In spite of the natural low sensitivity of deuterium, there is no doubt that, by taking advantage of higher magnetic field NMR spectrometers, it should be possible to acquire NAD spectra with shorter experimental times or determine enantiomeric excesses to a higher precision.<sup>6</sup> Indeed the  $S/N$  ratio is proportional to  $(B_0)^{3/2}$  for a given experimental time  $t_{\text{exptl}}$  while  $t_{\text{exptl}}$  is proportional to  $(B_0)^3$  for a given  $S/N$  ratio. To illustrate this, Fig. 8 shows the relationship between the total experimental time  $t_{\text{exptl}}$  and the  $S/N$  ratio with respect to values calculated with our 9.4 T spectrometer. Thus, when

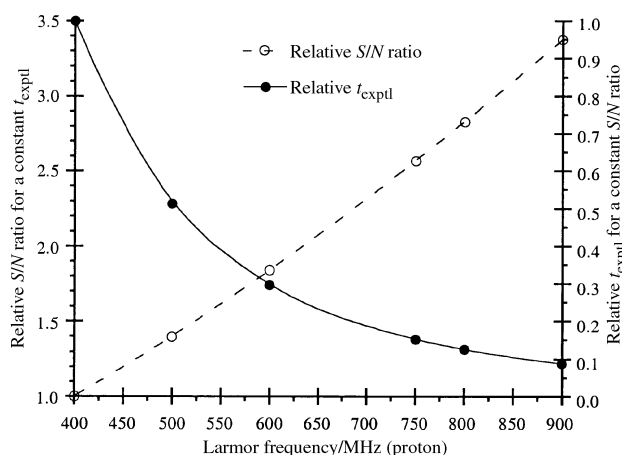


**Fig. 8** Evolution of the relative  $S/N$  ratio and the relative  $t_{\text{exptl}}$  as a function of the Larmor frequency with respect to a 9.4 T (400 MHz for proton) spectrometer. The reference value at 400 MHz is 1.

recording the NAD spectra of ( $\pm$ )-CP at 122.8 MHz (18.8 T), the  $S/N$  ratios would be increased by a factor of 2.8 for the same  $t_{\text{exptl}}$ . Conversely, the  $t_{\text{exptl}}$  would be reduced by a factor of 8 to obtain the same  $S/N$  ratio that is obtained at 400 MHz. This, incidentally, means that the  $S/N$  ratio of 20 measured here for the methyl group on the NAD spectra of ( $\pm$ )-CP would become *ca.* 60 at 18.4 T under the same experimental conditions. Such a  $S/N$  ratio would then result in an acceptable error in the determination of enantiomeric excesses. Another and probably cheaper solution to improve the  $S/N$  ratio of NAD spectra would consist in using selective, deuterium cryogenic probes. Indeed the present developments and studies of such cryoprobes have shown a very significant gain of the signal sensitivity (a factor 3 to 4) compared with standard high resolution probes.<sup>54</sup> Consequently the use of both higher field and deuterium cryoprobes should quickly establish that NAD 2D NMR spectroscopy is the most general and powerful technique for analysing chiral molecules in PBLG.

### Comparison of the various analytical potentialities of each technique

To compare and discuss the analytical potentialities of these various natural abundance NMR approaches, we have reported their respective features in terms of NMR and enantiomeric analysis in Table 1. Each of these NMR tools possesses advantages and drawbacks in terms of resolution, signal sensitivity, data presentation, complexity of spectral analysis, quality of chiral discrimination and accuracy in enantiomeric measurements. The choice of the technique to be used depends therefore on both chemical as well as NMR features of the chiral molecule (size of the molecule, functional groups, isolated group of nuclei, hybridization state of carbons, equivalent nuclei in deuterated isotopomers, ...) and the available amount of material under investigation in comparison with its molecular weight.

Although too large a number of interacting protons in the molecule yields generally unresolved, overcrowded  $^1\text{H}$  spectra in PBLG and prevents their analysis, it is always worthwhile to record such spectra to detect any separation of enantiomers through a difference in the residual  $^1\text{H}\text{-}^1\text{H}$  dipolar couplings for small, chiral, functionalized molecules (which are usually precursors of larger target molecules) or compounds having isolated groups far removed from other protons in the molecule. Indeed for such compounds, we may expect well resolved spectral patterns for both enantiomers, allowing the ee to be measured to a high accuracy.

For larger molecules, proton-decoupled carbon-13 NMR spectroscopy is an excellent alternative to  $^1\text{H}$  NMR since it prevents overcrowded carbon-13 NMR spectra. The spectra are relatively easy to analyse and the measurement of ee values is possible and reliable<sup>40,41</sup> with a reasonable amount of compound. However when  $^{13}\text{C}\{-^1\text{H}\}$  NMR fails by a lack of spectral resolution or negligible DOEs, the proton-coupled carbon-13 NMR can provide a useful alternative, in particular, for chiral derivatives exhibiting an isolated group (such as a methyl group) in the molecule. Finally, whilst noting the problem of deuterium sensitivity, NAD 2D NMR spectroscopy seems particularly well adapted for medium to large, functionalised or non-functionalised, chiral molecules because of the strong sensitivity of the quadrupolar interaction toward the DOE and the relatively simple analysis of 2D Q-COSY spectra.

Pragmatically, it is clear that chiral molecules possessing  $\text{sp}^2$  or  $\text{sp}$  carbons have a strong probability to be differentiated using  $^{13}\text{C}\{-^1\text{H}\}$  NMR with a satisfactory accuracy (*ca.* 5%) on the measurement of enantiomeric excess while no significant chiral discrimination would be expected to occur for chiral, non-functionalised molecules such as alkanes or cycloalkanes; conversely, NAD 1D and 2D NMR spectroscopy seems to be

**Table 1** Comparative table of various natural abundance NMR experiments for the chiral analysis in PBLG phases using a high resolution 400 MHz spectrometer

Nuclei observed	Natural isotopic abundance (%)	NMR sequence used	Useful anisotropic observables	Spectral analysis	Sensitivity to chiral differentiation	Signal sensitivity	Required amount for a racemic mixture <sup>c</sup> /mg	Average experimental time <sup>c</sup> /h	Estimated error on ee (%)
<sup>1</sup> H	99.9	1D S.P.A. <sup>a</sup>	<sup>1</sup> H- <sup>1</sup> H dipolar couplings	Difficult or impossible <sup>b</sup>	Low	Very high	2–10	<0.5	<5
<sup>13</sup> C	1.1	1D S.P.A. <sup>a</sup>	<sup>13</sup> C- <sup>1</sup> H dipolar couplings	Simple to difficult	Low to good	Low	20–60	2–8	5–10
<sup>13</sup> C- <sup>1</sup> H	1.1	1D S.P.A. <sup>a</sup>	<sup>13</sup> C CSA	Simple	Low to good	Low to high	20–50	1–4	3–5
<sup>13</sup> C- <sup>13</sup> C	0.012	2D (INADEQUATE)	<sup>13</sup> C- <sup>13</sup> C dipolar couplings	Simple to difficult	Very low	Very low	80–100	12–15	15–20
<sup>2</sup> H- <sup>1</sup> H	0.015	1D S.P.A. 2D (Q-COSY)	<sup>2</sup> H quadrupolar splittings	Simple	Strong	Very low	50–100	12–15	10–15

<sup>a</sup> S.P.A. = single pulse-acquisition sequence. <sup>b</sup> Impossible when the line broadenings give unresolved spectra. <sup>c</sup> Values assuming that the MW of enantiomers to be studied is in the range 100–200.

more adapted for such compounds for which <sup>13</sup>C-<sup>1</sup>H NMR is of less value. Indeed we may assume that the difference in the interactions between *S* and *R* isomers and the polypeptide will generate a rather small DOE and consequently only a very sensitive order-dependent NMR interaction such as the quadrupolar interaction may reveal an enantiomeric discrimination.<sup>55</sup> In addition, if the chiral molecule possesses magnetically equivalent deuterons (a methyl group), we may reach an adequate *S/N* ratio using a reasonable quantity of chiral material after an overnight acquisition. Although to date the accuracy on the measurements of enantiomeric excesses for reasonable signal-to-noise ratios are not better than 10%, the obtained experimental results already provide a very valuable estimation of ee values. In addition this technique allows a rapid and simple determination of the best site of chiral discrimination in the molecule and subsequently, may aid in selection of the most suitable synthetic strategy for introducing a deuteron in the molecule.

For all possible anisotropic natural abundance NMR techniques in PBLG the advantages of using higher magnetic field and/or a cryoprobe are obvious both in terms of chemical shift dispersion and *S/N*, the main benefit resulting in the higher precision in the calculation of ee values. We may expect that the approaches described here provide a very reliable alternative to current analytical techniques in the isotropic phase.

## Conclusion

The differentiation and the study of enantiomers is a challenging task. In this field, multinuclear NMR spectroscopy in the PBLG phase provides an efficient and convenient analytical tool to differentiate almost all possible enantiomers. The major interest of this methodology is that the polypeptide helices are able to interact enantioselectively with almost all enantiomers and give sufficiently large orientational differences to be revealed by almost all the routine NMR tools. In addition, the advent of routine high magnetic fields has made possible the observation of nuclei with very low sensitivity with acceptable *S/N* ratios such as deuterium at the natural abundance level. Here, we have shown, as illustrative examples, that it is possible to discriminate the *S* and *R* isomers of (±)-1-chloropropan-2-ol using proton, carbon-13 and deuterium spectroscopy on a single NMR sample. For almost all of the NMR methods reviewed, quantitative determination of enantiomeric purity is possible with a sufficient accuracy from simple peak integration. Nevertheless, each technique described here possesses both advantages and drawbacks in terms of signal sensitivity, complexity of spectral analysis, quality of chiral discrimination and accuracy in measurements of ee values. The choice of the best NMR technique for a given compound will depend on both the chemical and NMR features of the chiral molecule and

obviously the available amount of material. This choice, however, does not exclude the examination of other possible NMR techniques in PBLG when the results obtained are not convincing. In comparison to other NMR methods for chiral discrimination, the use of this emerging methodology offers therefore important advantages in terms of flexibility and versatility and provides a useful new NMR analytical tool. Besides, it has the valuable advantage that no labelling or any chemical modification of the chiral material is needed and the NMR requirements are not different compared to those for other isotropic methods.

This analytical method, characterized by its simplicity and adequate sensitivity, should certainly be considered as a powerful alternative to classical chiroptical, chromatographic or other NMR techniques. In this review, we have attempted to point out that this non-familiar tool for organic chemists is probably the most general method for the purpose of enantiomeric analysis. Finally, there is no doubt that by routinely taking advantage of higher magnetic field NMR spectrometers and/or using double tuned (carbon-13 and deuterium) cryogenic probe systems, the present potentialities of all these techniques should become evident and definitely establish the significant advantages of this strategy in the very near future.

In order to further evaluate the applicability, advantages and limitations of this methodological approach, additional work is still required and is currently being undertaken.

## Acknowledgements

We gratefully thank Professor J. W. Emsley and Professor A. Loewenstein for stimulating discussions.

## Notes and references

- 1 D. Parker, *Chem. Rev.*, 1991, **91**, 1441.
- 2 D. Parker and R. J. Taylor, *Asymmetric Synthesis*, Chapman and Hall, University Press, Cambridge, 1992.
- 3 A. Meddour, I. Canet, A. Loewenstein, J. M. Péchiné and J. Courtieu, *J. Am. Chem. Soc.*, 1994, **116**, 9652.
- 4 I. Canet, J. Courtieu, A. Loewenstein, A. Meddour and J. M. Péchiné, *J. Am. Chem. Soc.*, 1995, **117**, 6520.
- 5 A. Meddour, P. Berdagué, A. Hedli, J. Courtieu and P. Lesot, *J. Am. Chem. Soc.*, 1997, **119**, 4502.
- 6 D. Merlet, B. Ancian, J. Courtieu and P. Lesot, *J. Am. Chem. Soc.*, 1999, **121**, 5249.
- 7 E. E. Sackmann, S. Meiboom and L. C. Snyder, *J. Am. Chem. Soc.*, 1968, **90**, 2183.
- 8 E. E. Sackmann, S. Meiboom, L. C. Snyder, A. E. Meixner and R. E. Dietz, *J. Am. Chem. Soc.*, 1968, **90**, 3567.
- 9 P. Lesot, Y. Gounelle, D. Merlet, A. Loewenstein and J. Courtieu, *J. Phys. Chem.*, 1995, **99**, 14871; (correction), 1995, **100**, 14569.
- 10 P. Lesot, D. Merlet, T. P. Rantala, J. Jokisaari, J. W. Emsley and J. Courtieu, *J. Phys. Chem. A*, 1997, **101**, 5719.
- 11 J. W. Emsley and J. C. Lindon, *NMR Spectroscopy Using Liquid Crystal Solvents*, Pergamon Press, Oxford, 1975.

- 12 M. Jakubcova, A. Meddour, J. M. Péchiné, A. Baklouti and J. Courtieu, *J. Fluorine Chem.*, 1997, **86**, 149.
- 13 E. Graf, R. Graf, M. W. Hosseini, C. Huguenard and F. Taulelle, *Chem. Commun.*, 1997, 1459.
- 14 E. Lafontaine, J. P. Bayle and J. Courtieu, *J. Am. Chem. Soc.*, 1989, **111**, 8294.
- 15 J. Courtieu, E. Lafontaine, J. M. Péchiné and C. L. Mayne, *Liq. Cryst.*, 1990, **7**, 293.
- 16 P. Lesot, D. Merlet, A. Loewenstein and J. Courtieu, *Tetrahedron Asymmetry*, 1998, **9**, 1871.
- 17 K. Tabayashi and K. Akasaka, *Liq. Cryst.*, 1998, **1**, 127.
- 18 C. L. Khetrapal, K. V. Ramanathan, N. Suryaprakash and S. Vivekanandan, *J. Magn. Reson.*, 1998, **135**, 265.
- 19 A. Elliot and E. J. Ambrose, *Discuss. Faraday Soc.*, 1950, **9**, 246.
- 20 C. Robinson, *Trans. Faraday Soc.*, 1956, **52**, 571.
- 21 C. Robinson, *Mol. Cryst.*, 1966, **1**, 467.
- 22 K. Czarniecka and E. T. Samulki, *Mol. Cryst. Liq. Cryst.*, 1981, **63**, 205.
- 23 A. L. Lehninger, *Biochemistry*, Worth Publishers, Inc, New York, 1978.
- 24 P. Doty, J. H. Bradbury and A. M. Holtzer, *J. Am. Chem. Soc.*, 1956, **78**, 947.
- 25 L. Pauling, R. B. Corey and H. R. R. Brandson, *Proc. Natl. Acad. Sci.*, 1951, **37**, 205.
- 26 T. J. McMaster, H. J. Carr, M. J. Miles, P. Cairns and V. J. Morris, *Macromolecules*, 1991, **24**, 1428.
- 27 M. Panar and W. D. Phillips, *J. Am. Chem. Soc.*, 1968, **90**, 3880.
- 28 E. T. Samulski and A. V. Tobolsky, *Macromolecules*, 1968, **1**, 155.
- 29 P. Doty, J. H. Bradbury and A. M. Holtzer, *J. Am. Chem. Soc.*, 1956, **78**, 947.
- 30 J. C. Mitchell, A. E. Woodward and P. Doty, *J. Am. Chem. Soc.*, 1957, **79**, 3955.
- 31 C. Canlet, D. Merlet, P. Lesot, A. Meddour, A. Loewenstein and J. Courtieu, *Tetrahedron: Asymmetry*, 2000, **11**, 1911.
- 32 P. Lesot, D. Merlet, A. Meddour, A. Loewenstein and J. Courtieu, *J. Chem. Soc., Faraday Trans.*, 1995, **91**, 1371.
- 33 H. O. Kalinowski, S. Berger and S. Braun, *Carbon-13 NMR Spectroscopy*, Wiley and Sons, Chichester, 1984.
- 34 E. H. Hardy, R. Witt and M. D. Zeidler, *J. Magn. Reson.*, 1998, **134**, 300.
- 35 E. R. Blout, R. H. Karlson, P. Doty and B. Hargitay, *J. Am. Chem. Soc.*, 1954, **76**, 4492.
- 36 E. R. Blout and R. H. Karlson, *J. Am. Chem. Soc.*, 1954, **76**, 941.
- 37 R. Albert, J. Danklmaier, H. Honig and H. Kandolf, *Synthesis*, 1987, 635.
- 38 A. J. Shaka, J. Keeler and R. Freeman, *J. Magn. Reson.*, 1983, **53**, 335.
- 39 The simulation program 'PANIC' is marketed by Bruker SA.
- 40 V. Madiot, P. Lesot, D. Gree, J. Courtieu and R. Gree, *Chem. Commun.*, 2000, 169.
- 41 O. Dirat, C. Kouklovsky, Y. Langlois, P. Lesot and J. Courtieu, *Tetrahedron: Asymmetry*, 1999, **10**, 3197.
- 42 R. R. Ernst, G. Bodenhausen and A. Wokaun, *Principles of Nuclear Magnetic Resonance in One and Two Dimensions*, Clarendon Press, Oxford, 1987.
- 43 G. Wagner and E. R. P. Zuiderweg, *Biochem. Biophys. Res. Commun.*, 1983, **113**, 854.
- 44 G. Otting and K. Wütrich, *J. Magn. Reson.*, 1986, **66**, 359.
- 45 A. Bax, *Two-dimensional Nuclear Magnetic Resonance in Liquids*, Delft University Press, Dordrecht, Holland, 1984.
- 46 D. Sandstrom, K. T. Summamen and M. H. Levitt, *J. Am. Chem. Soc.*, 1994, **116**, 9357.
- 47 J. P. Bayle, J. Courtieu, E. Gabetty, A. Loewenstein and J. M. Péchiné, *New J. Chem.*, 1992, **16**, 837.
- 48 I. Canet, A. Meddour, J. Courtieu, J. L. Canet and J. Salatiin, *J. Am. Chem. Soc.*, 1994, **116**, 2155.
- 49 W. Smadja, S. Auffret, P. Berdagué, D. Merlet, C. Canlet, J. Courtieu, J. Y. Legros, A. Boutros and J. C. Fiaud, *Chem. Commun.*, 1997, 2031.
- 50 D. Merlet, B. Ancian, W. Smadja, J. Courtieu and P. Lesot, *Chem. Commun.*, 1998, 2301.
- 51 D. Merlet, M. Sarfati, B. Ancian, J. Courtieu and P. Lesot, *Phys. Chem. Chem. Phys.*, 2000, **2**, 2283.
- 52 R. Freeman, *A Handbook of Nuclear Magnetic Resonance*, A. W. Longman Limited, Essex, 2nd edn., 1997, p. 258.
- 53 A. Belguise, *Analisis*, 1995, **23**, M57.
- 54 Y. W. Kim, W. L. Earl and R. E. Norberg, *J. Magn. Reson.*, 1995, **116**, 139.
- 55 M. Sarfati, J. Courtieu and P. Lesot, *Chem. Commun.*, 2000, 1113.